Structure and Function of Skeletal Muscle in Zebrafish Early Larvae

Ying Dou,[1] Monika Andersson-Lendahl,[2] and Anders Arner[1]

[1]Department of Physiology and Pharmacology and [2]Department of Medical Nutrition, Karolinska Institutet, Stockholm, Sweden

Zebrafish muscles were examined at an early developmental stage (larvae 5–7 d). Using aluminum clips, preparations (~1.5 mm length, 150 μm diameter) were mounted for force registration and small angle x-ray diffraction. Sarcomeres were oriented mainly in parallel with the preparation long axis. Electrical stimulation elicited fast and reproducible single twitch contractions. Length–force relations showed an optimal sarcomere length of 2.15 μm. x-ray diffraction revealed clear equatorial 1.1/1.0 reflections, showing that myofilaments are predominantly arranged along the preparation long axis. In contrast, reflections from older (2 mo) zebrafish showed two main filament orientations each at an ~25° angle relative to the preparation long axis. Electrical stimulation of larvae muscles increased the 1.1/1.0 intensity ratio, reflecting mass transfer to thin filaments during contraction. The apparent lattice volume was 3.42×10^{-3} μm^3, which is smaller than that of mammalian striated muscle and more similar to that of frog muscles. The relation between force and stimulation frequency showed fusion of responses at a comparatively high frequency (~186 Hz), reflecting a fast muscle phenotype. Inhibition of fast myosin with *N*-benzyl-*p*-toluene sulphonamide (BTS) showed that the later phase of the tetanus was less affected than the initial peak. This suggests that, although the main contractile phenotype is fast, slow twitch fibers can contribute to sustained contraction. A fatigue stimulation protocol with repeated 220 ms/186 Hz tetani showed that tetanic force decreased to 50% at a train rate of 0.1 s^{-1}. In conclusion, zebrafish larvae muscles can be examined in vitro using mechanical and x-ray methods. The muscles and myofilaments are mainly orientated in parallel with the larvae long axis and exhibit a significant fast contractile component. Sustained contractions can also involve a small contribution from slower muscle types.

The Journal of General Physiology

INTRODUCTION

During the last decade the zebrafish, *Danio rerio*, has been introduced as an important model for the study of developmental biology. Key advantages of this vertebrate system are that the embryos and early larvae stages are transparent and develop rapidly, that the zebrafish reproduce easily, and that orthologous genes in the zebrafish and humans regulate similar developmental processes (Langenau and Zon, 2005). Specific mutated zebrafish strains are available and genetic tools such as morpholino oligonucleotide injection can be applied to the zebrafish model and enable gene expression to be blocked during early stages of development. Since the zebrafish develop several organ functions within the first week, effects of morpholino oligonucleotide knockdown on phenotype can be analyzed comparatively rapidly (Nasevicius and Ekker, 2000; Sumanas and Larson, 2002). These properties of the zebrafish and the improved methods for manipulating gene expression and inducing targeted mutations have led to increased use of the zebrafish, not only as a model for the evaluation of specific gene function but also as a model of human disease.

In the field of muscle research, studies on development of zebrafish have provided insight into the molecular genetic mechanisms that regulate the initial development and differentiation of muscle cells. Different populations of slow and fast muscle precursors have been identified (Devoto et al., 1996). Proteins such as UNC-45b and obscurin are found to play important roles in assembly, structural support, and in sarcomeric alignment of striated myofibrils in the zebrafish (Raeker et al., 2006; Wohlgemuth et al., 2007). Furthermore, the zebrafish has been used in the study of molecular mechanisms involved in human skeletal muscular dystrophy, dilated cardiomyopathy and hypertrophic cardiomyopathy (Seeley et al., 2007).

Most of the previous studies on zebrafish muscle have analyzed genetic, histological, and molecular aspects with a developmental focus. Neural control of motor activity in zebrafish larvae has been examined using kinematic studies of swimming patterns (McDearmid and Drapeau, 2006). However, studies of muscle function in the zebrafish are currently very sparse or lacking. In particular, the characterization of muscle function in the zebrafish larvae would be important since this developmental stage is accessible for genetic modification, including morpholino oligonucleotide knockdown. Such experiments would enable functional consequences of specific muscle genes to be analyzed in a vertebrate system with comparatively high throughput. In this study we have therefore developed a novel method to analyze

Correspondence to Anders Arner: Anders.Arner@ki.se

Abbreviations used in this paper: BTS, *N*-benzyl-*p*-toluene sulphonamide; DTE, dithioerythritol; EDL, extensor digitorum longus.

The Rockefeller University Press $30.00
J. Gen. Physiol. Vol. 131 No. 5 445–453
www.jgp.org/cgi/doi/10.1085/jgp.200809982

the mechanical function and the myofilament structure of zebrafish larvae muscle. We report functional and structural data showing that the zebrafish larvae muscles and myofibrils are predominantly arranged in parallel with the larvae long axis, have an optimal sarcomere length at ~2.15 μm, and exhibit characteristics of fast muscle types with low fatigue resistance.

Part of these results has been presented in preliminary form (Dou, Y., M. Andersson-Lendahl, and A. Arner. 2008. *J. Muscle Res. Cell Motil.* doi:10.1007/s10974-008-9127-z.)

MATERIALS AND METHODS

Zebrafish Early Larvae Preparation and Mounting for Mechanical Experiments

Zebrafish early larvae (*Danio rerio*, Tübingen strain), 5–7 d old, were obtained from the Karolinska Institutet Zebrafish Facility. The experiments were approved by the ethical committee and conformed with the *Guide for the Care and Use of Laboratory Animals* (1996. National Academy of Sciences, Washington D.C.). At this developmental stage, the fish have reached the larvae stage, are ~3 mm long, and exhibit short burst-like swimming behavior. The larvae were held in E3 medium (5 mM NaCl, 0.17 mM KCl, 0.33 mM $CaCl_2$, and 0.33 mM $MgSO_4$, pH 6.8–6.9). Prior to experiment a larva was transferred to E3 medium containing 0.017% tricaine (3-amino benzoic acid ethylester). When the larva was anesthetized, the head was crushed and the preparation mounted as illustrated in Fig. 1 A. The clips were made of thin aluminum foil. These were folded at 45° angles to trap the head and the tail portions of the larvae, providing a defined and stable attachment. Small holes were made in the aluminum foil for attaching the preparation between the extended arm of an AE801 force transducer (Capto as) and a fixed pin for length adjustment using a micrometer screw. For mechanical experiments the preparation was mounted horizontally in a 0.5-ml Perspex organ bath at room temperature (22°C). The bath was perfused with modified Krebs-Henseleit solution of the following composition (in mM): 117.2 NaCl, 25.2 $NaHCO_3$, 4.7 KCl, 1.2 $MgCl_2$, 1.2 KH_2PO_4, 2.5 $CaCl_2$, 11.1 glucose gassed with 5% CO_2/95%O_2 (pH 7.4). The bath is equipped with a glass window that enables observation of the preparation and sarcomere patterns with an inverted microscope (Nikon Eclipse TE300). Pictures were captured using a CCD camera. Stimulation was performed via two platinum electrodes placed on either side of the preparation using a Grass S48 stimulation unit and a current amplifier. The force signal was recorded (10 kHz sampling frequency) using an AD-converter (PowerLab, ADInstruments).

Mechanical Experiments

The preparations were activated using electrical field stimulation with 0.5-ms pulse duration. In each experiment the applied voltage was varied to give maximal single twitch contractile responses and the preparation was subsequently stimulated at supramaximal intensity (~20% above maximal). Length–force relationships were determined in preparations stimulated with single twitches at ~2-min intervals. The preparations were stretched between stimuli, and at each length the force (active and passive) and the sarcomere length (from CCD camera pictures) were determined. The sarcomere length was determined in the muscles of the trunk. The optimal length was defined as the sarcomere length giving maximal active single twitch tension. The relation between active force and stimulation frequency was determined in preparations stretched to optimal length and stimulated with 220-ms stimulation trains at 8-min intervals. The stimulation frequency was increased in steps (in the range 20–200 Hz). The initial peak response and the sustained tension at 220 ms were determined. To examine the role of different myosin types, experiments were performed with repeated 220-ms trains at 186 Hz (giving fused tetani) at different concentrations (0, 0.5, 1, 2, 3, and 4 μM) of the myosin inhibitor *N*-benzyl-*p*-toluene sulphonamide (BTS) (Cheung et al., 2002). Muscle fatigue properties were recorded using repeated 220-ms tetani (186 Hz, supramaximal voltage at optimal length). Starting with stimulation at 8-min intervals (train rate 0.0021 s^{-1}), where responses could be repeated without loss of tension, the interval between stimulation trains was gradually shortened to obtain the following train rates: 0.0042 (4-min interval), 0.014, 0.032, 0.054, 0.08, 0.127, and 0.3 s^{-1}. In these experiments the force after 220 ms stimulation was determined and related to the maximal force obtained at 8-min stimulation intervals.

Small Angle x-ray Diffraction

Small angle x-ray diffraction patterns were recorded using synchrotron radiation at beamline A2 (HASY laboratory at DESY Hamburg). The preparations were mounted horizontally as described above between two fixed hooks in a ~200-μl bath, equipped with Kapton windows at 22°C. Sarcomere length was determined using light diffraction from a HeNe laser. The focus of the x-ray beam was elongated (~1.5 mm) in the horizontal direction, along the preparation long axis, and with a width in the vertical direction of ~0.2 mm. The camera length was 2.9 m and the two-dimensional patterns were recorded using a MarCCD detector (MarResearch). The equatorial patterns were analyzed using Quantity one software (Bio-Rad Laboratories, Inc.) and calibrated with collagen samples (dried rat tail tendon). The preparations were held in either E3 medium (composition see above) or, for the majority of the experiments, in a MOPS-buffered physiological solution of the following composition (in mM): 118 NaCl, 24 MOPS, 5 KCl, 1.2 $MgCl_2$, 1.2 Na_2HPO_4, 1.6 $CaCl_2$, 10 glucose (pH 7.4), equilibrated with air. To record equatorial patterns using the detector system above recording times of 10–120 s were used. Two parallel platinum wires were inserted into the cuvette for electrical stimulation as described above. Relaxed and contracted patterns were recorded by opening the beam shutter either during relaxation or during 1-s tetanic (186 Hz) stimulations. In these experiments the total recording time was 1–2 s (sum of two contractions).

Chemically Permeabilized Preparations

Zebrafish larvae were permeabilized for 3 h at room temperature in a relaxation solution containing (in mM) 30 imidazole (pH 7.0), 5 EGTA, 11.61 MgAcetate, 10 ATP, 20 KMethansulfonate, 12.5 phosphocreatine, 1 dithioerythritol (DTE), and 0.5 mg/ml creatine kinase, with 0.1% Triton X-100 added. Thereafter, the preparations were stored at −20°C in a solution containing (in mM) 5 ATP, 4 EGTA, 30 imidazole (pH 7.0), 5 $MgCl_2$, 2 DTE, 50% glycerol. In x-ray diffraction studies, comparisons were made with permeabilized preparations of 2-mo-old zebrafish. These were anaesthetized with Tricain and killed by crushing the head. The skin was removed and the tissue was chemically skinned as above. For comparison of Ca^{2+} sensitivity, mouse extensor digitorum longus (EDL) muscles were permeabilized. These preparations were held at the approximate in situ length and permeabilized for 24 h at 4°C in a solution containing (in mM) 5 EGTA, 2.5 ATP, 2.5 MgAcetate, 30 TES, 170 K-Propionate at pH 7.0. The muscle bundles were stored in the same solution with addition of 50% glycerol. In experiments on permeabilized muscles, the preparations were mounted in the relaxation solution (composition see above,

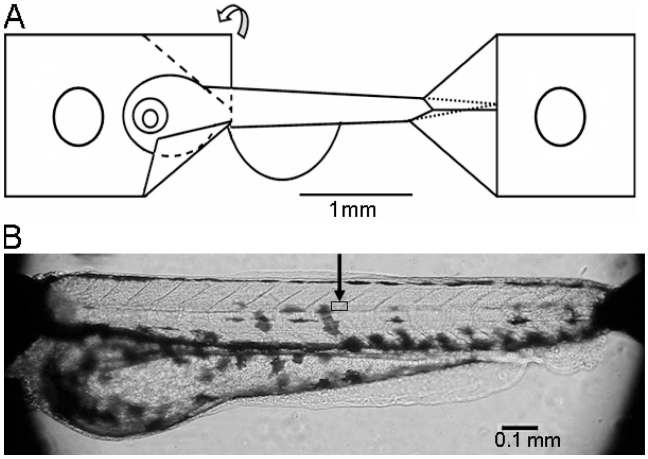

Figure 1. Zebrafish larvae preparation. (A) Schematic illustration of preparation attachment using aluminum foil clips at both ends of the larvae. The aluminum foil is folded along the dashed lines as shown on the left clip. A small hole is made in each clip for mounting. (B) Photograph of the preparation mounted on the microscope stage. The square area under the arrow indicates the approximate location of the area examined with higher magnification light microscopy in Fig. 2 A.

without Triton X-100) at 22°C and stretched to a low passive tension. The muscles were then contracted with contraction solution made by replacing EGTA with CaEGTA in the relaxation solution. To determine the Ca^{2+} sensitivity, the preparations were exposed to solutions with increasing Ca^{2+} concentrations, obtained by varying the ratio of CaEGTA/EGTA.

Statistical Analysis

Data are shown as mean ± SEM. Statistical analysis was performed using Student's *t* test. All statistics and curve fitting were performed using software implemented in SigmaPlot 2002, SPSS Co.

RESULTS

General Properties of the Preparation

As seen in Fig. 1, aluminum foil clips were used to mount the zebrafish early larvae preparations for isometric force recording and for structural studies. The preparations were ∼1.7 mm long, between the tips of the aluminum clips. The length of the larvae is ∼2.7 mm. The region between the clips spans from caudally of the head approximately at the location of the heart to ∼0.4 mm from the tip of the tail. Illustrations of zebrafish larvae at this developmental stage can be found in Nixon et al. (2005). The main muscular parts of the larvae (above the swim bladder, the yolk sack, and abdominal regions seen in the preparation of Fig. 2 B) were ∼150 µm in diameter. We usually kept the abdominal parts of the larvae, as seen in photograph of Fig. 1, in order to minimize mechanical manipulation of the preparations. We could however not observe any changes in the mechanical responses if these parts were removed. The regularly arranged myosepta at an ∼45° angle against the larva long axis are clearly seen at the dorsal side (Fig. 1 B).

Mechanical Responses and Length–Force Relationships

Regular sarcomere patterns were observed in the dorsal muscles with the light microscope and were found to be oriented mainly in parallel with the preparation long axis and the notochord (Fig. 2 A). Note that the myoseptum is arranged at an angle relative to the long axis (arrow in photograph). The unstimulated larvae were relaxed and pulse stimulations (0.5 ms pulse duration) resulted in rapid muscle twitches (Fig. 2 B). The half-time for contraction and relaxation of the single twitches

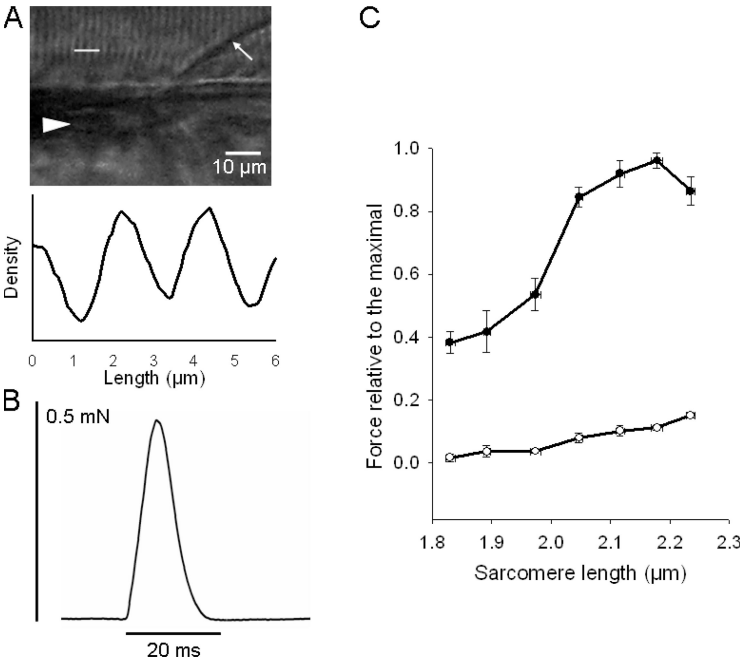

Figure 2. Sarcomere pattern, single twitch contraction and length force relationships. (A) High magnification photograph showing sarcomere patterns and the corresponding density record from the segment indicated with the white line in the photograph. Arrow indicates myoseptum, triangle indicates notochord. The approximate location of this area is indicated in Fig. 1 B showing a picture from a similar preparation. (B) Original recording of a single twitch elicited by electrical stimulation. (C) Relationship between sarcomere length and passive (open circles) and active (filled circles) force. Force values are expressed relative to the maximal active force, $n = 7$.

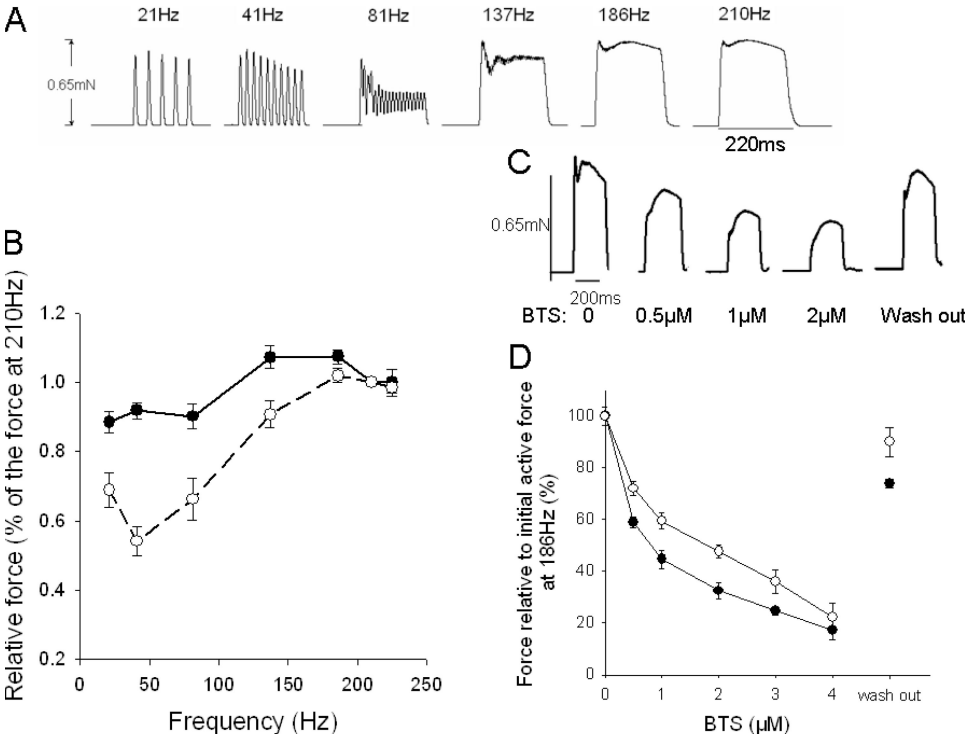

Figure 3. (A) Original recording of 220-ms tetani elicited at different stimulation frequencies; (B) force–frequency relationship (initial peak, filled circles; tetanic force, open circles); (C) Representive tetanic contractions (stimulation frequency, 186 Hz) with or without BTS; (D) BTS sensitivity of the initial peak (filled circles) and tetanic force (open circles) and the recovery after washout, $n = 6$.

were 3.2 ± 0.2 ms and 4.7 ± 0.2 ms, respectively ($n = 9$). These single twitches could be repeated at least 10–20 times without any loss of force, using 2-min intervals. Shorter intervals resulted in reduced force development. The mechanical experiments were performed in the modified Krebs-Henseleit solution. Contractions could also be elicited in the E3 medium, but the contractions were less reproducible with a gradual loss of force, most likely due to damage of the fish skin by the mounting procedure and subsequent osmotic effects. We also examined contractions in a frog Ringer solution (in mM): 115.5 NaCl, 2 KCl, 2 Na_2HPO_4 /NaH_2PO_4 (pH 7.0), and 1.8 $CaCl_2$, gassed with air. Under these conditions the contractions were slightly weaker than those in the Krebs-Henseleit solution. Since the single twitch stimulation in Krebs-Henseleit solution gave reproducible and near maximal activation (see Fig. 3 below) we used this mode of activation to determine the length–force relationship. As seen in Fig. 2 C, the relation between sarcomere length and active force was bell shaped with ascending and descending limbs. The optimal length for active tension development was on average 2.15 ± 0.02 μm ($n = 7$). The passive tension at optimal length was 12.8 ± 1.4% ($n = 7$) of the maximal active single twitch tension. Stretch above the optimal length resulted in lower active force. This decreased force was not due to an irreversible damage since active force increased again when the muscle was shortened back to the optimal length. Information on longer sarcomere length (>2.25 μm) is limited since at this degree of stretch the preparation stiffness became very high and the preparation slipped in the attachment points. The maximal active single twitch force developed by the zebrafish larvae at optimal length was 0.46 ± 0.06 mN ($n = 7$).

Force–Frequency Relationship

An original recording of a larva preparation stimulated with 220-ms tetani at different frequencies is shown in Fig. 3 A. Individual twitches, with almost full relaxation in between, were observed at stimulation frequencies up to ∼40 Hz. At this frequency the second twitch was somewhat enhanced, compared with the single twitch, and the last (10th) was slightly decreased, suggesting an initial potentiation phenomenon and a subsequent fatigue. At ∼80 Hz, twitches started to fuse, with incomplete relaxation in between, and at ∼190 Hz, a complete fusion was observed. At higher frequencies the force responses had an initial peak and a second more sustained component. An initial contraction peak was observed within 10–20 ms after onset of stimulation. This initial peak was similar to the single twitch force and was slightly increased at higher frequencies. The tetanic force was measured as the second force peak during the later phase of the tetanic contractions (∼50 ms after stimulation for frequencies >137 Hz). At the lower frequencies (<137 Hz) the tetanic force was measured as force at the end of the tetanus. Fig. 3 B summarizes the frequency force data. The initial peak reached a maximal value, ∼25% above single twitch force, at 137–186 Hz. Tetanic force was lower than single twitch force at low stimulation frequencies and reached a maximal value, similar to the initial peak, at ∼190 Hz.

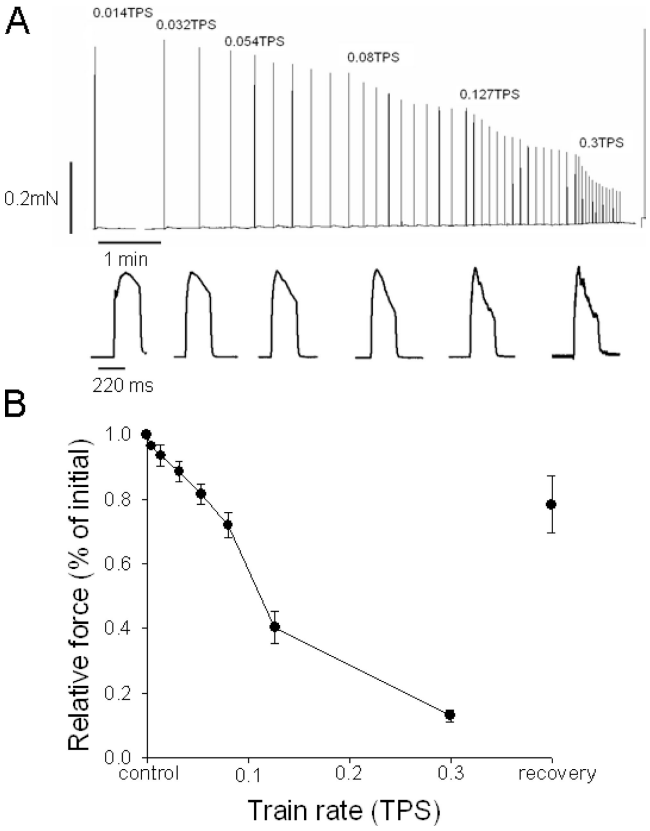

Figure 4. (A) Original force recording of zebrafish larvae preparation stimulated with short tetani at increased train rate (top). Representative individual tetanic force responses at the different train rates are displayed below in the bottom panel. To show the shape of the contractions in the records the peak forces were scaled to similar amplitude. Absolute force amplitude is displayed in the top panel. (B) Mean values of tetanic force at different train rates (trains per second), $n = 9$.

To examine if the different phases of the tetanic contractions reflected contributions from different muscle fiber types we determined the effects of BTS (0–4 μM). This compound is reported to be an inhibitor of fast myosin isoforms (Cheung et al., 2002). As seen in Fig. 3 (C and D), BTS inhibited both the initial peak and the tetanic force, but with different potency. The effect of BTS was reversible to a large extent as illustrated in C and D. The initial peak was inhibited at lower concentrations. Curve fits of a hyperbolic equation to force (y) and BTS concentration (c) data ($y = 1 - c^h/(c^h + EC_{50}{}^h)$) showed that the initial component had a significantly ($P < 0.01$) lower EC_{50} value compared with the tetanic tension with similar slope h-parameter (initial, EC_{50}: 0.8 ± 0.1, h: 0.92 ± 0.08; tetanic tension, EC_{50}: 1.5 ± 0.1 μM, h: 1.03 ± 0.13, $n = 6$).

Fatigue Resistance

To explore the fatigue resistance of the zebrafish larvae muscles, the preparations were activated with repeated 220-ms tetanic stimulations at increasing train rate as shown in top trace of Fig. 4 A. We evaluated the tetanic tension. It was not possible to distinguish the initial peak at higher train rates (bottom trace in Fig. 4 A). The tetanic force decreased gradually at increasing train rate and fell rapidly at train rates between 0.08 and 0.127 s^{-1}. The shape of the tetanic contractions changed at increasing train rate and became less well maintained. The force decrease was reversible and when the train rate was returned to one stimulus every 8 min, a substantial recovery was observed (Fig. 4).

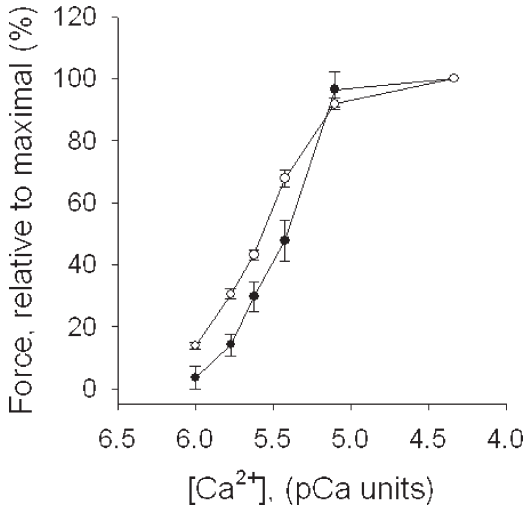

Figure 5. Ca^{2+} sensitivity of permeabilized zebrafish larvae (filled circles, $n = 8$) preparations and mouse EDL preparations (open circles, $n = 6$). $[Ca^{2+}]$ is given in pCa units (pCa = −log $[Ca^{2+}]$, for $[Ca^{2+}]$ in M).

Calcium Sensitivity of Contraction

The maximal tension of the permeabilized zebrafish preparations was ∼20% of the force of the intact muscle. The force could not be improved by skinning at lower temperature (4°C) or by using higher Triton X-100 concentrations (0.3–1%) or using the EGTA/glycerol treatment applied to the EDL muscles. The calcium sensitivity of force was examined in chemically permeabilized zebrafish preparations and, for comparison, in mouse EDL preparations. Fig. 5 shows summarized data for active force at different free $[Ca^{2+}]$. The relation was shifted toward higher Ca^{2+} concentrations in zebrafish larvae preparations compared with mouse EDL preparations. Force (y) and $[Ca^{2+}]$ (c) data were analyzed using a hyperbolic equation: $y = c^h/(c^h + EC_{50}{}^h)$. The EC_{50} (in pCa units) and the h-parameter values were 5.42 ± 0.05 and 2.57 ± 0.15 in zebrafish larvae preparations, and 5.57 ± 0.02 and 1.97 ± 0.07 in mouse EDL preparations. Both the EC_{50} and h values were significantly different between the muscle types ($P < 0.05$).

Equatorial x-ray Diffraction Patterns

Fig. 6 shows a recording of equatorial patterns from an unstimulated intact larva preparation (A and B) in

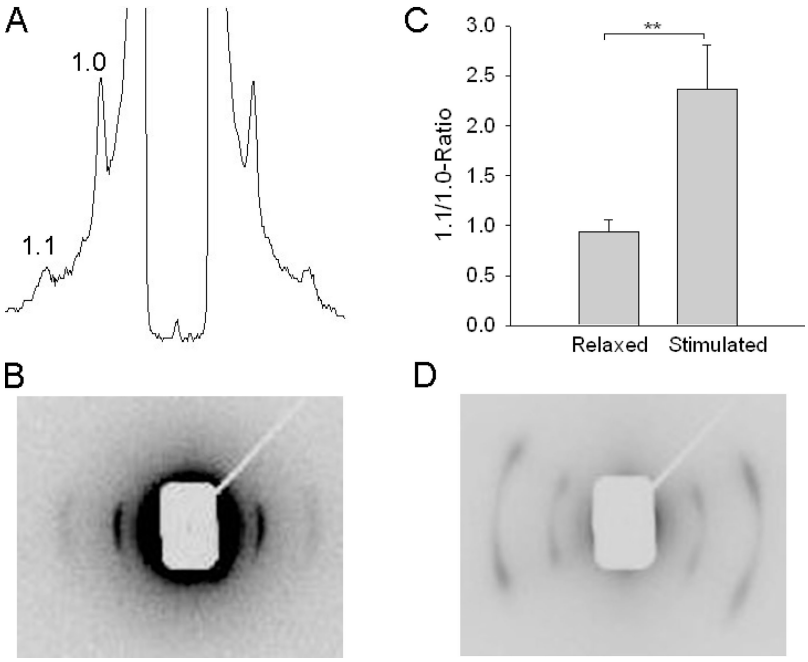

Figure 6. Equatorial x-ray diffraction patterns. (A) Equatorial pattern of a relaxed zebrafish larvae in E3 medium. The 1.0 and 1.1 reflections are indicated. (B) The corresponding two-dimensional image recorded. (C) The 1.1/1.0 intensity ratio in relaxed and stimulated zebrafish larvae preparations in MOPS-buffered medium ($n = 7$). (D) Two-dimensional image of a permeabilized 2-mo-old zebrafish in relaxing medium. In B and D, the equator, i.e., the direction perpendicular to the preparation axis, is oriented horizontally (recording time 15 s).

E3 medium. Clear 1.1 and 1.0 reflections are observed. The meridional patterns and layer lines were not observed using the beam focus and exposure times in the present experiments. The reflections were oriented perpendicular to the preparation, suggesting that the myofilaments are mainly arranged with a mean direction in parallel with the preparation long axis. For comparison we recorded patterns from permeabilized relaxed adult (2 mo old) zebrafish preparations (Fig. 6 D). In this tissue the equatorial patterns was not oriented in parallel with the preparation, but showed two clear orientations each at an angle of 26.2 ± 0.7 ($n = 11$) degrees relative to the equator and preparation long axis. In the larvae muscles the mean values for the 1.1 and 1.0 lattice spacing in E3 medium was 24.5 ± 0.2 and 42.9 ± 0.2 nm ($n = 11$), respectively. Since the mechanical parameters were better maintained in physiological solution we also determined the spacing in MOPS-buffered physiological medium. In this medium the lattice spacing values were smaller (1.1: 22.5 ± 0.2 and 1.0: 39.3 ± 0.2 nm, $n = 7$), which can be attributed to the different osmolarities of the solutions (E3 medium 14 mosm/liter vs. 306 mosm/liter the MOPS-buffered physiological medium). In these experiments, the sarcomere length of the preparations was determined using laser diffraction and the muscles were stretched to 1.9 μm sarcomere length. We also varied the sarcomere length in the range 1.8–2.1 μm. The equatorial spacing was dependent on the sarcomere length (for the 1.0-reflection the spacing was 40.3 ± 0.4, 38.8 ± 0.3, 38.6 ± 0.3, and 38.3 ± 0.2 nm, $n = 6$–9, at the sarcomere lengths 1.8, 1.9, 2.0, and 2.1 μm). The fish larvae preparations could not be stretched over a larger range, but using these data for the 1.0 spacing (d_{10}) and sarcomere length we calculated the apparent lattice volume per sarcomere ($=(2/\sqrt{3}) \times d^2_{10} \times$ sarcomere length (Millman, 1998) to 3.42×10^{-3} μm^3). To further examine if the 1.0 and 1.1 reflections were influenced by mass transfer between thick and thin filaments we recorded the relative intensities in the relaxed state and in muscles stimulated during 2 × 1 s (186 Hz). Under these conditions the average force during the recording was ~40% of maximal. In the stimulated preparations the 1.1 peak remained essentially unchanged whereas the 1.0 peak decreased markedly. The ratio of the 1.1/1.0 intensities was calculated after background subtraction and integration of the respective peak areas. Fig. 6 C shows that the ratio increased in stimulated muscles.

DISCUSSION

We report on a novel method to examine zebrafish muscle at an early developmental stage (larvae 5–7 d), using a mechanical set-up and low angle x-ray diffraction. We present novel structural and functional data of the muscles in this model organism.

Many aspects of the link between specific genes and muscle physiology and/or disease have been examined in the mammalian system using transgenic mouse technologies and in nonvertebrate systems, e.g., the fruit fly, *Drosophila melanogaster*, and the nematode, *Caenorhabditis elegans*. The vertebrate zebrafish, which now has a characterized genome, offers obvious advantages such as high reproductive capacity with short generation time and rapid development. Powerful genetic techniques, including microinjection of antisense morpholino oligonucleotides, can be applied to the zebrafish model. Since the fish develop rapidly and the antisense knockdown

is transient, a time window of ~1 wk is useful for genetic/functional studies using this approach. We therefore focused on the 5–7-d larva stage when the fish has a developed musculature and starts to swim. The musculature at this developmental stage is mainly organized in somites along the back of the fish (van Raamsdonk et al., 1982). The muscle cells are arranged between the myosepta, which are considered to be attachment points for muscle fibers (Henry et al., 2005). Since it was not possible to prepare intact single fibers for the detailed mechanical analysis, we used the whole larvae body comprising the body muscles in the preparation. The calcification of the axial skeleton in the trunk region does not appear until 7 d post fertilization (Du et al., 2001), which allows us to stretch the preparation and record force generation without obvious restriction from the skeletal system. In addition, the transparency of the larvae enables the sarcomere pattern to be visualized and analyzed using microscopy and recorded with laser light diffraction. The force recordings were not affected by the presence of the gut and swim bladder and we routinely kept these in the preparation. Although the skin was not removed, the preparation enabled access to the contractile filament environment, since compounds (e.g., BTS) influenced contraction when added to the bath solution.

Microscopic observation of the larvae preparations revealed that the majority of muscle cells in the back muscles had visible sarcomere patterns and were oriented mainly in parallel with the long-axis of the preparation, although the myosepta were arranged at an ~45° angle. The equatorial x-ray pattern also showed that the myofilaments were arranged with a mean direction in parallel with the long axis of the preparation. This is in contrast with the arrangement in the 2-mo-old fish where two main muscle orientations were identified. A previous study of zebrafish larvae (van Raamsdonk et al., 1982) has shown a very thin superficial layer of fibers of embryonic red type and a deeper layer of white type fibers. The superficial fibers were mainly in parallel whereas the deeper fibers were more helically arranged. Our x-ray and light microscopy data would reflect mainly the bulk of white fibers and suggest that the angle in the helical arrangement is small and that the two main directions of muscles in the adult fish are not established in the 5–7-d larvae. The 1.1 and 1.0 reflections of the larvae were comparatively strong and, although the focus of this investigation was on relaxed muscle measurements we found that activation with electrical stimulation resulted in changes of the 1.1 and 1.0 intensities characteristic of myosin cross-bridge movement toward the thin filaments. In this series of experiments we could not resolve an increase in the 1.1 intensity during contraction, which could reflect that the mean active force was lower than maximal during the recording. The constant volume behavior during stretch could not be examined in detail, since the range of sarcomere length changes was limited. However, the lattice spacing (for 1.0: 39.3 nm at sarcomere length 1.9 μm) and the calculated lattice volume (3.42×10^{-3} μm^3) at 306 mOsm were smaller than values reported for mammalian striated muscle and more similar to those of the frog (Millman, 1998), suggesting a more dense packing of myofilaments in the zebrafish larvae compared with the mammalian muscle.

Active tension of the larvae muscles was dependent on sarcomere length, exhibiting a length–tension relationship with an ascending and a descending limb. The optimal sarcomere length was determined to 2.15 μm. The optimal length of the zebrafish muscles was similar to that reported for frog muscles (Altringham and Bottinelli, 1985) and shorter than that of mammalian fast twitch muscles (mouse flexor digitorum brevis: 2.1–2.4 μm, Edman, 2005). As discussed below, the predominant part of the muscle mass is composed of fast fiber types and our data for optimal muscle length are similar to those reported for fast twitch fibers of the perch (between 1.9 and 2.2 μm; Granzier et al., 1991), and smaller than those of slow twitch fibers from the same animal (between 2.6 and 2.8 μm). In straight carp Rome and Sosnichi (1991) have reported that the sarcomere length of unfixed frozen white and red muscle were 1.96 and 2.06, respectively (Rome and Sosnicki, 1991), although these data were not related force generation.

In most fish, sustained swimming utilizes slow muscle fibers (also known as red muscle) whereas escape responses are powered by fast muscle fibers (white muscle, Rome and Sosnicki, 1991). In the adult zebrafish, the fast muscle fibers occupy deep portion of the body and the slow muscle fibers are located in wedge-shaped region between the skin and the superficial cells (van Raamsdonk et al., 1982). In the larger carp, the anatomical arrangement of the red and white muscles differs. During the more extensive backbone bending, occurring in escape responses, the white muscles can operate over a sarcomere length range where they generate significant tension. In contrast the red muscles are shortened to sarcomere lengths where active tension is lower, and they are thus more important in swimming with less tail bending (Rome and Sosnicki, 1991). In the zebrafish larvae, the majority of the muscles are mainly arranged in parallel with the long axis of the fish and have characteristics of fast twitch fibers with regard to optimal sarcomere length and contractile properties (see below). They do not have the anatomical advantage for force development of an angled arrangement.

We report that the contractile responses of the zebrafish larvae have the characteristics of a comparatively fast muscle type. The fusion frequency of the contractions was 186 Hz, which is higher than that of fast

mammalian and frog muscle fibers and close to that reported for swim bladder muscle (fusion frequency is 250–300 Hz; Rome et al., 1996). The single twitch response appeared to fatigue quickly at increasing frequencies, already in trains when the twitch contractions did not fuse. Consistent with a faster muscle phenotype the force–[Ca^{2+}] relationship was shifted toward higher [Ca^{2+}] compared with mouse EDL, suggesting a low Ca^{2+} sensitivity (Stephenson and Williams, 1982). The decreased Ca^{2+} sensitivity could reflect that the Ca^{2+} dissociation rate from troponin in the zebrafish muscle is rapid, which could be important for the fast contraction and relaxation. During sustained tetanic stimulations we found two components (an initial and a sustained) in the force responses of the zebrafish larvae preparations. It is possible that these two parts include different contribution of fast and slow muscle fibers in the preparations. The experiments using BTS, which is considered to be selective for fast skeletal myosin with minor effects on cardiac and slow skeletal muscle (Cheung et al., 2002), revealed that the later phases of tetanic contractions were less inhibited. This suggests that more sustained contractions, when the fast fibers fatigue, can recruit a component of force from a small population of slower fiber types. The larvae have a major component of deep muscle fibers of a white muscle type and a thin outer layer of fibers designated embryonic red (van Raamsdonk et al., 1982). It is possible that the two contractile components discussed above reflect the contribution from these two muscle fiber types. If we estimate the cross-sectional area of the larvae from our measurements of preparation width and published information on the shape of the cross section, we obtain an approximate force per preparation cross-sectional area of 35–50 mN/mm^2 for the single twitch. This is lower than values reported for force per cell area in single fibers of mouse and frog (Edman, 2005). Our estimate is however influenced by the relative amount of muscle in the cross section and the mechanical coupling of the cells, and an extrapolation to force per cell cross section in the zebrafish larvae muscle is therefore currently not possible.

The zebrafish larvae preparations displayed a rapid force reduction in a repeated tetani fatigue model, with a significant force reduction already at a low train rate of 0.1 s^{-1}. Several studies on mouse models indicate that the force decline during fatiguing contractions is related to a reduced Ca^{2+} release with metabolic origin (Westerblad et al., 1998). As discussed above, zebrafish muscles are fast and most likely require a rapid calcium release and reuptake during its ordinary contractile activity, and it is therefore possible that the repeated activity can put a significant strain on the Ca^{2+} release mechanisms and cell metabolism.

In conclusion, we have characterized a system for recording muscle function and structure of zebrafish at the larvae developmental stage. We report that the muscles and myofilaments are mainly longitudinally orientated in parallel with the larvae long axis, exhibiting a significant fast contractile component. Sustained contractions can also involve a small contribution from slower muscle types.

The study was supported by the Swedish Research Council (C1359 to Anders Arner).

Kenneth C. Holmes served as editor.

Submitted: 4 February 2008
Accepted: 26 March 2008

REFERENCES

Altringham, J.D., and R. Bottinelli. 1985. The descending limb of the sarcomere length-force relation in single muscle fibres of the frog. *J. Muscle Res. Cell Motil.* 6:585–600.

Cheung, A., J.A. Dantzig, S. Hollingworth, S.M. Baylor, Y.E. Goldman, T.J. Mitchison, and A.F. Straight. 2002. A small-molecule inhibitor of skeletal muscle myosin II. *Nat. Cell Biol.* 4:83–88.

Devoto, S.H., E. Melancon, J.S. Eisen, and M. Westerfield. 1996. Identification of separate slow and fast muscle precursor cells in vivo, prior to somite formation. *Development.* 122:3371–3380.

Du, S.J., V. Frenkel, G. Kindschi, and Y. Zohar. 2001. Visualizing normal and defective bone development in zebrafish embryos using the fluorescent chromophore calcein. *Dev. Biol.* 238:239–246.

Edman, K.A. 2005. Contractile properties of mouse single muscle fibers, a comparison with amphibian muscle fibers. *J. Exp. Biol.* 208:1905–1913.

Granzier, H.L., H.A. Akster, and H.E. Ter Keurs. 1991. Effect of thin filament length on the force-sarcomere length relation of skeletal muscle. *Am. J. Physiol.* 260:C1060–C1070.

Henry, C.A., I.M. McNulty, W.A. Durst, S.E. Munchel, and S.L. Amacher. 2005. Interactions between muscle fibers and segment boundaries in zebrafish. *Dev. Biol.* 287:346–360.

Langenau, D.M., and L.I. Zon. 2005. The zebrafish: a new model of T-cell and thymic development. *Nat. Rev. Immunol.* 5:307–317.

McDearmid, J.R., and P. Drapeau. 2006. Rhythmic motor activity evoked by NMDA in the spinal zebrafish larva. *J. Neurophysiol.* 95:401–417.

Millman, B.M. 1998. The filament lattice of striated muscle. *Physiol. Rev.* 78:359–391.

Nasevicius, A., and S.C. Ekker. 2000. Effective targeted gene "knockdown" in zebrafish. *Nat. Genet.* 26:216–220.

Nixon, S.J., J. Wegner, C. Ferguson, P.F. Mery, J.F. Hancock, P.D. Currie, B. Key, M. Westerfield, and R.G. Parton. 2005. Zebrafish as a model for caveolin-associated muscle disease; caveolin-3 is required for myofibril organization and muscle cell patterning. *Hum. Mol. Genet.* 14:1727–1743.

Raeker, M.O., F. Su, S.B. Geisler, A.B. Borisov, A. Kontrogianni-Konstantopoulos, S.E. Lyons, and M.W. Russell. 2006. Obscurin is required for the lateral alignment of striated myofibrils in zebrafish. *Dev. Dyn.* 235:2018–2029.

Rome, L.C., and A.A. Sosnicki. 1991. Myofilament overlap in swimming carp. II. Sarcomere length changes during swimming. *Am. J. Physiol.* 260:C289–C296.

Rome, L.C., D.A. Syme, S. Hollingworth, S.L. Lindstedt, and S.M. Baylor. 1996. The whistle and the rattle: the design of sound producing muscles. *Proc. Natl. Acad. Sci. USA.* 93:8095–8100.

Seeley, M., W. Huang, Z. Chen, W.O. Wolff, X. Lin, and X. Xu. 2007. Depletion of zebrafish titin reduces cardiac contractility by disrupting the assembly of Z-discs and A-bands. *Circ. Res.* 100:238–245.

Stephenson, D.G., and D.A. Williams. 1982. Effects of sarcomere length on the force-pCa relation in fast- and slow-twitch skinned muscle fibres from the rat. *J. Physiol.* 333:637–653.

Sumanas, S., and J.D. Larson. 2002. Morpholino phosphorodiamidate oligonucleotides in zebrafish: a recipe for functional genomics? *Brief. Funct. Genomics Proteomics.* 1:239–256.

van Raamsdonk, W., L. van't Veer, K. Veeken, C. Heyting, and C.W. Pool. 1982. Differentiation of muscle fiber types in the teleost *Brachydanio rerio*, the zebrafish. Posthatching development. *Anat. Embryol. (Berl.).* 164:51–62.

Westerblad, H., D.G. Allen, J.D. Bruton, F.H. Andrade, and J. Lannergren. 1998. Mechanisms underlying the reduction of isometric force in skeletal muscle fatigue. *Acta Physiol. Scand.* 162:253–260.

Wohlgemuth, S.L., B.D. Crawford, and D.B. Pilgrim. 2007. The myosin co-chaperone UNC-45 is required for skeletal and cardiac muscle function in zebrafish. *Dev. Biol.* 303:483–492.